



Utilization of aluminium buffing dust as a raw material for the production of mullite

Nuntaporn KONGKAJUN¹, Benya CHERDHIRUNKORN¹, Warunee BORWORNKIATKAEW², and Parinya CHAKARTNARODOM^{3,*}

¹ Department of Materials and Textile Technology, Faculty of Science and Technology, Thammasat University, Klong Luang, Pathum Thani, 12120, Thailand

² National Metal and Materials Technology Center, Pathum Thani, 12120, Thailand

³ Department of Materials Engineering, Faculty of Engineering, Kasetsart University, Bangkok, 10900, Thailand

*Corresponding author e-mail: fengpryc@ku.ac.th

Received date:
30 September 2018
Revised date:
15 October 2018
Accepted date:
23 March 2019

Keywords:
Mullite
Aluminium buffing dust
Refractory

Abstract

Aluminium buffing dust is a by-product from fine polishing process in aluminium part manufacture. Because of its high content of aluminium, alumina and silica, this waste could be used to prepare refractory mullite. Aluminium buffing dust and Ranong kaolin were mixed with the ratio of 100: 0 to 40:60 by ball milling. The batch mixtures were shaped by dry pressing. The green specimens were fired at temperature in the range of 1100-1400°C. The physical properties such as bulk density and water absorption were done by Archimedes principle. Phase analysis was observed by X-ray diffraction (XRD). Microstructural characterization was done by scanning electron microscopy (SEM). Modulus of rupture of the sintered samples were characterized by 3-point bending test. The results showed the specimen prepared from the batch mixture ratio of 60:40 and sintered at 1400°C has highest bulk density of 2.71 g·cm⁻³ and bending strength of 60 MPa.

1. Introduction

Aluminosilicate-based ceramics such as mullite (3Al₂O₃·2SiO₂) have been used in high temperature application due to their low thermal expansion, high temperature stability, good chemical resistance and high temperature mechanical strength. Mullite-based materials are generally used as refractory such as kiln furniture and electronic applications [1-2]. To prepare mullite, solid state reaction of aluminosilicates at high temperature is generally required by mixing of powder compounds such as oxide or hydroxide of aluminium and silicon according to the chemical formula of mullite [3-7]. The utilization of clays such as kaolin is the most attractive way for mullite fabrication at relatively low cost. Mullite and silica are formed by thermal decomposition of kaolinite (>1200°C). However, there is not enough proportion of alumina to complete mullitization at higher temperature (>1300°C). Thus, this silica can be mullitized by adding alumina-rich raw materials.

In metal part manufacturer, the fine polishing process causes buffing residue [8]. The large amount of the buffing residue produced from aluminium industry needs the costs for disposal. The previous study of the preparation of cordierite ceramic from the buffing residue was reported [9]. This waste consists of major proportion of aluminium, alumina and silica that could be used for serving as a source of alumina to obtain mullite. To date, there were many works on fabricating mullite ceramics and other glass-ceramics from many kinds of wastes [10-19]. The recycling of this industrial waste is environmentally valuable not only preventing improper disposal in the environment but also reducing the production cost.

Thus, the objective of present work was to fabricate mullite ceramic refractory by blending aluminium buffing dust with inexpensive natural raw materials such as Ranong kaolin. The phase structural and crystal morphology of fired samples was studied by X-ray diffraction (XRD) and scanning electron microscopy (SEM). Bulk density and water absorption were conducted by Archimedes principle. Bending test was used to measure the mechanical strength of samples.

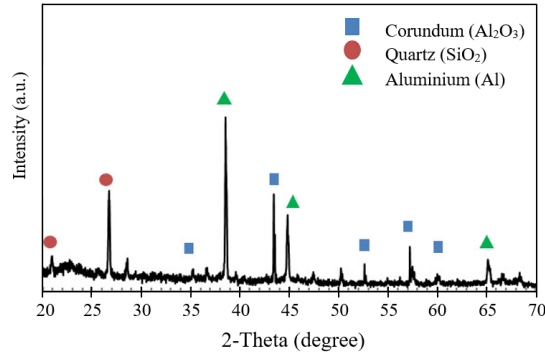
2. Experimental

2.1 Raw materials

The results of chemical composition of starting materials analyzed by X-ray Fluorescence (XRF: Rigaku) were given in Table 1. The major components of aluminium buffing dust were Al₂O₃ (63.3 wt%) SiO₂ (19.1 wt%) MgO (2.63 wt%) and Fe₂O₃ (2.7 wt%). There were also small amount of alkali and alkaline-earth metal oxides such as K₂O (2.6 wt%) and CaO (0.5 wt%). The Phase composition of aluminium buffing dust was analyzed by X-ray Diffractometer (XRD: Bruker D8 Advance, 40 kv, 40 mA) as seen in Figure 1. The XRD pattern indicated that the main phases of aluminium buffing dust were aluminium (Al), corundum (Al₂O₃) and quartz (SiO₂). Before preparing the batch mixtures, as-received aluminium buff was calcined at 600°C in air for getting rid of the volatile compound. The thermogravimetric analyzes (TG/DTA) of aluminium buffing dust was detected by using TA instrument SDT 2950 simultaneous thermal analyzer (TG/DTA) operating at 1400°C in air.

Table 1. The Chemical composition of aluminium buffing dust and Ranong kaolin.

	Oxide (wt%)								
	Al ₂ O ₃	SiO ₂	MgO	Fe ₂ O ₃	TiO ₂	CaO	Na ₂ O	K ₂ O	LOI
Al buffing dust	63.5	19.1	2.63	2.7	0.50	0.54	-	0.18	10.83
Ranong kaolin	33.0	54.0	0.2	0.5	0.1	0.3	2.0	0.2	9.6

**Figure 1.** XRD pattern of aluminium buffing dust.

2.2 Experimental procedure

Aluminium buffing dust and Ranong kaolin were weighed and mixed according to the batch mixture as listed in Table 2. The batch compositions mixed with the ratio of aluminium buffing dust to Ranong kaolin were from 100:0 to 40:60. The batch mixtures were blended by wet ball milling for 8 h and then dried in a drying oven at 100°C for 24 h. The green specimens were compacted by uniaxial dry pressing under 100 MPa. The shaped specimens then were fired at the different temperatures (ranging from 1100 to 1400°C in air). Firing cycles correspond to heating and cooling rate of 5°C·min⁻¹ and 2 h soaking in air at maximum temperature.

Table 2. The composition of experimental formula (wt%).

Sample no.	Raw materials	
	Aluminium buffing dust (wt%)	Ranong kaolin (wt%)
A100	100	0
A80	80	20
A60	60	40
A50	50	50
A40	40	60

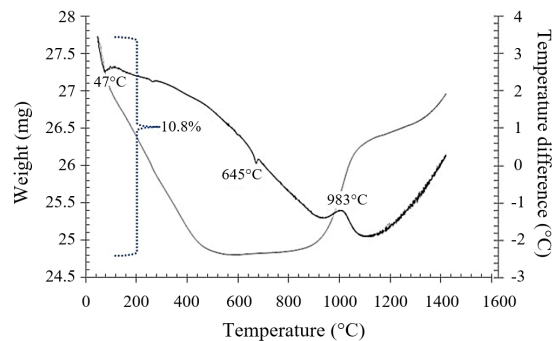
Bulk density and water absorption of fired specimens were determined by conventional method using Archimedes principle. Phase analysis of fired specimens was examined by XRD (Bruker D8 Advance). Microstructural analysis (SEM- Hitachi S-3400N equipped with EDS) of fired bodies was observed. The three-point bending test (Tinius Olsen Universal Testing Machine) was performed at ambient

temperature. The geometry of test specimens was 8 mm x 5 mm x 80 mm. The specimen testing data were the averages of five specimens for each group.

3. Results and discussion

3.1 Thermal analysis of raw materials

The thermogravimetric analysis (TG/DTA) of aluminium buffing dust was shown in Figure 2. The DTA curve of the sample showed endothermic peaks at temperatures of 47°C and 250°C. These peaks correspond to the removal of moisture and organic substance used during buffing process. The calculated total weight loss in this temperature range was about 11%. The endothermic peak at temperature of 645°C was detected without weight change which attributed to melting temperature of aluminium. It was also observed the exothermic peak at 983°C and weight gain which responded to oxidation of aluminium at high temperature.

**Figure 2.** TG/DTA curves of aluminium buffing dust.

3.2 Phase structure and microstructure of the sintered samples

X-ray diffraction patterns of the different mixtures at different temperatures were shown in Figure 3-4. After firing the mixture A100 at 1200°C, corundum phase was mainly detected along with cristobalite phase as seen in Figure 3. Corundum phase was derived from oxidation of aluminium in aluminium buffing dust. Cristobalite phase was expected from quartz in buffing compound. A small amount of mullite phase was also observed this indicated that some of corundum phase started to react with cristobalite for mullitization by solid-state reaction [3-6]. With the increase of the amount of kaolin in the mixtures (the samples A80 to A40), increasing amount of mullite

phase was detected. From the samples A60 to A40, the addition of kaolin enhanced the silica content to form mullite phase. However, small amount of cristobalite phase was still observed.

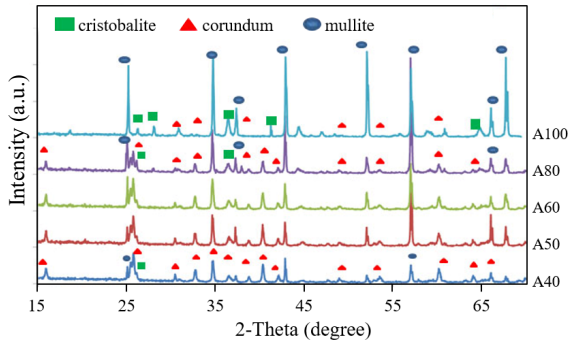


Figure 3. XRD pattern of various batch mixtures sintered at 1200°C.

The further increase of the firing temperatures up to 1400°C, the reaction among the constituents of the mixtures A60, A50 and A40 seemed to be completed forming mullite as primary phase comparable of the amounts of corundum phase as shown in Figure 4. The disappearance of cristobalite phase was also detected. The addition of aluminium buffering dust contributed the formation of corundum and cristobalite phase. The further increase in temperature caused and an enhancement in the intensity of mullite peaks and a reduction of corundum peaks. An absence of cristobalite

peaks indicated that it reacted with corundum to form mullite. Higher temperature enhanced in the solubility of mullite.

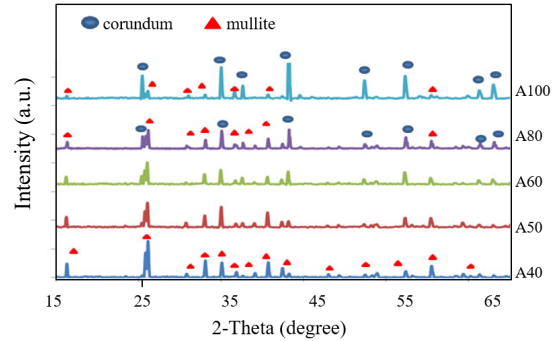


Figure 4. XRD pattern of various batch mixtures sintered at 1400°C.

Figure 5(a) and 5(b) showed SEM micrographs of the samples sintered at 1400°C. the rounded shaped grains of corundum were mainly observed in the high alumina-rich formulations (the sample A100 and A80) as observed in the XRD analysis (Figure 4). The elongated needle-like mullite crystal emerged as residual phase. Figure 5(c) showed SEM images of the high silica-rich formulations (the sample A60). The elongated grains of mullite were primary observed. With higher silica-rich compositions (the sample A50 and A40), the glassy phase was observed as seen in Figures 5(d) and 5(e).

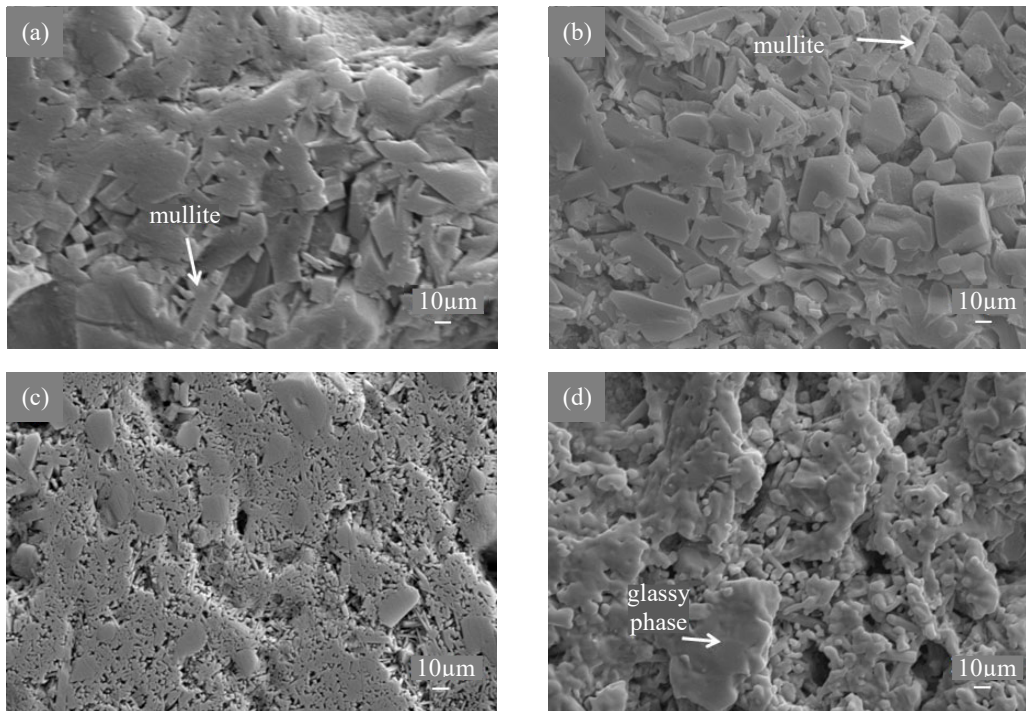


Figure 5. SEM micrograph of the samples sintered at 1400°C and prepared from the samples A100 (a), A80 (b), A60 (c), A50 (d) and A40 (e).

As reported by the literature, mullite was generated by the formation of a silica-rich liquid phase [14,20]. According to the $\text{Al}_2\text{O}_3\text{-SiO}_2$ binary phase diagram, liquid phase could be formed at above eutectic temperature (1590°C). In this study, a liquid phase appeared at a relatively low temperature (1400°C). The main reason was the presence of impurities such as iron oxide, alkali and alkaline oxide in the starting materials. These impurities also accelerated the alumina dissolution rate in silica-rich liquid phase to form mullite [12].

3.3 Physical properties of the sintered samples

The Plots of Bulk density and water absorption of the specimen batches as a function of sintering temperatures and batch formula were shown in Figure 6 and 7, respectively. Bulk density of all mixtures increased with increasing temperature. From 1300 to 1400°C , raising in the content of kaolin (the sample A60 to A40) considerably increased bulk density and decreased water absorption. This was because of enhancement of mullite phase by alumina dissolving into silica-rich liquid phase during sintering, which could promote the elimination of pores and densification of the samples.

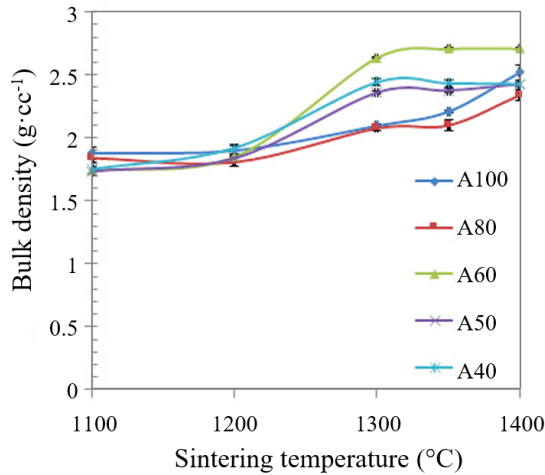


Figure 6. Bulk density of fired specimens at various mixtures.

Figure 8 showed the curves of the bending strength of the samples with different sintering temperatures. Bending strength of all mixtures showed an increasing trend with increasing sintering temperature. This indicated that sintering temperature influenced on strength by enhancing liquid formation and mullitization. The bulk density and bending strength of the sample A60 reached the highest bulk density of $2.71 \text{ g}\cdot\text{cm}^{-3}$ and bending strength of 60 MPa at 1400°C . The value of mechanical strength was close to the previous reports (40-70 MPa) using industrial wastes as a raw material and sintered in the range of $1400\text{-}1450^\circ\text{C}$ [11-13]. This indicated a potential for recycling aluminium

buffing dust as a raw material of refractory bodies such as commercial mullite-based saggars or plates [21].

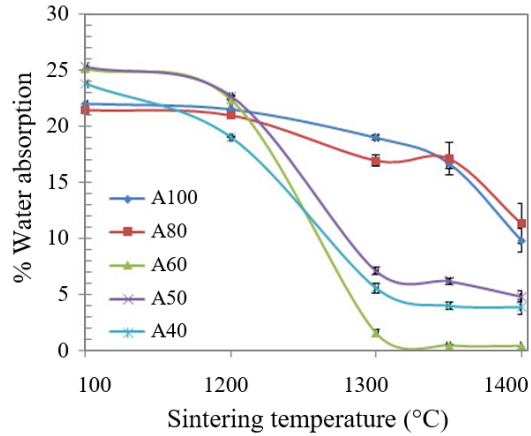


Figure 7. Water absorption of fired specimens at various mixtures.

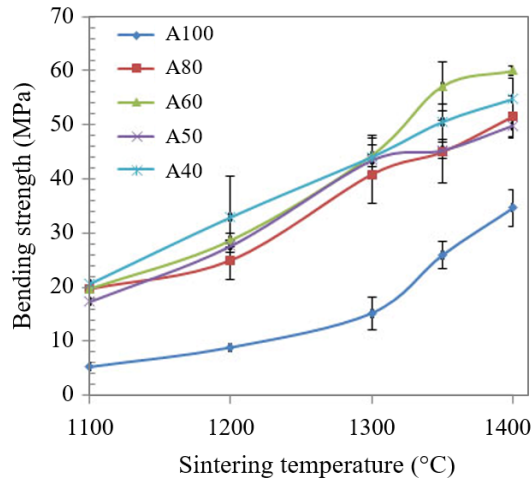


Figure 8. Bending strength of fired specimens at various mixtures.

Further increasing kaolin in the samples A50 and A40 sintered at 1400°C , bulk density and bending strength were lower than the mixture A60. The reasonable explanation of lower strength was the formation of glassier phases. The presence of glass phase could lower the bending strength as the strength of glass phase was generally lesser than that of mullite crystal. Moreover, presence of porosity in higher amount of kaolin in the formulation could be attributed to dehydroxylation of kaolinite during firing.

4. Conclusions

This work was to attempt to prepare low-cost mullite from an inexpensive starting material such as kaolin and the aluminium buffing dust from aluminium manufacturing. The batch mixture ratio of 60 wt%

aluminium buff and 40 wt% Ranong kaolin achieved the optimum properties when sintered at 1400°C, which had highest bulk density of 2.71 g·cm⁻³ and bending strength of 60 MPa. In the XRD analysis of the formulation, mullite was detected as a major phase. Moreover, the recycling of aluminium buffing dust is possible to obtain a new material such as mullite in order to reduce solid waste management cost.

5. Acknowledgements

This work was supported by Thammasat University Research Fund.

References

- [1] L. A. Akay, D. M. Dabbs, and M. Sarikaya, "Mullite for structural, electronic and optical applications," *Journal of American Ceramic Society*, vol. 74, pp. 2343-2354, 1991.
- [2] F. C. Zhang, H. H. Luo and S. G. Roberts, "Mechanical properties and microstructure of Al₂O₃/mullite composite," *Material Science*, vol. 42, pp. 6798-6802, 2007.
- [3] G. Chen, H. Qi, W. Xing, and N. Xu, "Direct preparation of macroporous mullite supports for membranes by in situ reaction sintering," *Journal of Membrane Science*, vol. 318, pp. 38-44, 2008.
- [4] Y.-F. Chen, M.-C. Wang, and M.-H. Hon, "Phase transformation and growth of mullite in kaolin ceramics," *Journal of the European Ceramic Society*, vol. 24, pp. 2389-2397, 2004.
- [5] C. Y. Chen, G. S. Lan, and W. H. Tuan, "Preparation of mullite by the reaction sintering of kaolinite and alumina," *Journal of the European Ceramic Society*, vol. 20, pp. 2519-2525, 2000.
- [6] S. C. Vieira, A. S. Ramos, and M. T. Vieira, "Mullitization kinetics from silica- and alumina-rich wastes," *Ceramics International*, vol. 33, pp. 59-66, 2007.
- [7] A. Esharghawi, C. Penot, and F. Nardou, "Contribution to porous mullite synthesis from clays by adding Al and Mg powders," *Journal of the European Ceramic Society*, vol. 29, pp. 31-38, 2009.
- [8] A. Dickman, "The science of scratches-polishing and buffing mechanical surface preparation," *Metal Finishing*, vol.105, pp. 13-29, 2007.
- [9] N. Kongkajun, P. Chakartnarodom, and W. Borwornkiatkaew, "The fabrication of refractory cordierite from aluminium buff mixture," *Key Engineering Materials*, vol. 690, pp. 97-102, 2016.
- [10] P. Appendino, M. Ferraris, I. Matekovits, and M. Salvo, "Production of glass-ceramic bodies from the bottom ashes of municipal solid waste incinerators," *Journal of the European Ceramic Society*, vol. 24, pp. 803-810, 2004.
- [11] M. J. Ribeiro and J. A. Labrincha, "Properties of sintered mullite and cordierite pressed bodies manufactured using Al-rich anodizing sludge," *Ceramic International*, vol. 34, pp. 593-597, 2008.
- [12] Y. Dong, X. Feng, X. Feng, Y. Ding, X. Liu, and G. Meng, "Preparation of low-cost mullite ceramics from natural bauxite and industrial waste fly ash," *Journal of Alloys and Compounds*, vol. 460, pp. 599-606, 2008.
- [13] H. P. A. Alves, J. B. Silva, L. F. A. Campos, S. M. Torres, R. P. S. Dutra, and D. A. Macedo, "Preparation of mullite based ceramics from clay-kaolin waste mixtures," *Ceramic International*, vol. 42, pp. 19086-19090, 2016.
- [14] V. J. Silva, M. F. Silva, W. P. Goncalves, R. R. Menezes, G. A. Neves, H. L. Lira, and L. N. L. Santana, "Porous mullite blocks with compositions containing kaolin and alumina waste," *Ceramic International*, vol. 42, pp. 15471-15478, 2016.
- [15] X. Xu, J. Li, J. Wu, Z. Tang, L. Chen, Y. Li, and C. Lu, "Preparation of thermal shock resistance of corundum-mullite composite ceramics from andalusite," *Ceramic International*, vol. 43, pp. 1762-1767, 2017.
- [16] P. J. Sanchez-Soto, D. Eliche-Quesada, S. Martinez-Martinez, E. Garzon-Garzon, L. Perez-Villarejo, and J. M. Rincon, "The effect of vitreous phase on mullite and mullite-based ceramic composites from kaolin wastes as by-products of mining, sericite clays and kaolinite," *Materials Letters*, vol. 223, pp. 154-158, 2018.
- [17] T. Sahraoui, H. Belhouchet, M. Heraiz, N. Brihi, and A. Guermat, "The effects of mechanical activation on the sintering of mullite produced from kaolin and aluminum powder," *Ceramic International*, vol. 42, pp. 12185-12193, 2016.
- [18] Z. Hou, C. Liu, L. Liu, and S. Zhang, "Microstructural evolution and densification behavior of porous kaolin-based mullite ceramic added with MoO₃," *Ceramic International*, vol. 44, pp. 17914-17918, 2018.
- [19] F. Chargui, M. Hamidouche, H. Belhouchet, Y. Jorand, R. Durfnoune, and G. Fantozzi, "Mullite fabrication from natural kaolin and aluminium slag," *Ceramica y Vidrio*, vol. 57, pp. 169-177, 2018.
- [20] H. P. Ji, M. H. Fang, Z. H. Huang, K. Chen, Y. G. Xu, Y. G. Liu, and J. T. Huang, "Effect of La₂O₃ additives on the strength and microstructure of mullite ceramics obtained from coal gangue and alpha-alumina," *Ceramic International*, vol. 39, pp. 6841-6846, 2013.
- [21] C. Sadik, I. E. E. Amrani, and A. Albizane, "Recent advances in silica-alumina refractory: A review," *Journal of Asian Ceramic Societies*, vol. 2, pp. 83-96, 2014.